JPE 7-4-5

A New High Efficiency PWM Single-Switch Isolated Converter

Ki-Bum Park †, Chong-Eun Kim *, Gun-Woo Moon * and Myung-Joong Youn *

†*Department of Electrical Engineering and Computer Science, KAIST, Korea

ABSTRACT

The flyback converter is one of the most attractive isolated converters in small power applications because of its simple structure. However, it suffers from high device stress, large transformer size, and high voltage stress across its switch and diode. To solve these problems a new cost-effective PWM single-switch isolated converter is proposed. The proposed converter has no output filter inductor, reduced voltage stress on the secondary devices, and reduced transformer size. Moreover, the switch turn-off loss is reduced and no dissipative snubber across the secondary diode is required. Therefore, it features a simple structure, a low cost, and high efficiency. The operational principle and characteristics of the proposed converter are presented and compared with the flyback converter and then verified experimentally.

Keywords: isolated converter, single-switch, flyback converter

1. Introduction

Until now, the various types of isolated switching mode power converters have been proposed [1-6]. Among them, the flyback converter shown in Fig. 1 is a favorite topology for its simple circuit configuration and easy isolation compared with other topologies in low power applications [4-6]. That is, with using only one switch, there is no output filter inductor and no additional transformer reset circuit, thereby making it very attractive. However, the flyback converter suffers from the high voltage/current stress of devices and the large magnetizing current of the transformer increases the transformer size. Moreover, the high primary peak current causes high switch turn-off loss and the leakage inductance of the transformer causes high voltage spike and ringing across the switch and diode at the switching transitions, which requires snubbers.

To improve the abovementioned drawbacks, a new cost-effective PWM single-switch isolated converter is proposed in this paper. As seen in Fig. 2, the proposed converter simply consists of switch Q, transformer T, capacitor C_S, diodes D_{S1} and D_{S2}, and an auxiliary snubber network. In the proposed converter, the small transformer leakage inductor L_{lkg} drives the powering current, therefore no large filter inductor is required. The reset of the transformer is automatically achieved by the secondary capacitor C_S and the offset magnetizing current of the transformer is less than that of the flyback converter, resulting in the smaller transformer size. In addition, the switch turn-off loss can be reduced by controlling the resonance between L_{lkg} and C_S. Furthermore, the voltage stresses of secondary diodes D_{S1} and D_{S2} are clamped to V_O, therefore resulting in basically less voltage stress with no snubber needed.

Manuscript received April 29, 2007; revised August 24, 2007
† Corresponding Author: parky@rainbow.kaist.ac.kr
Tel: +82-42-869-3475, Fax: +82-42-861-3475, KAIST
*Dept. of Electrical Engineering and Computer Science, KAIST

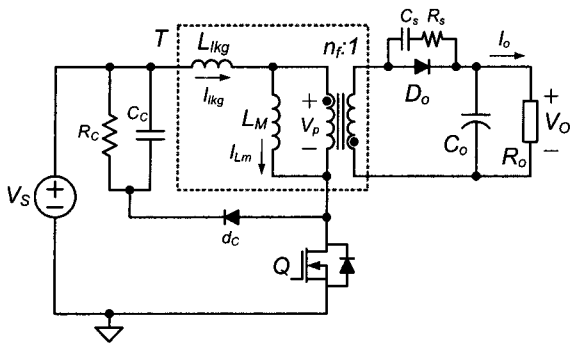

Fig. 1 Flyback converter

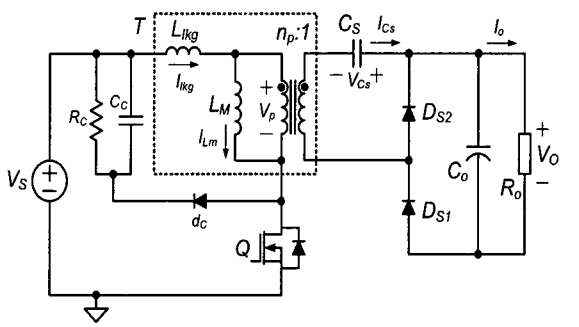

Fig. 2 Proposed converter

2. Operational Principle

The key waveforms and topological states of proposed converter are presented in Figs. 3 and 4, respectively. The operation of one switching period is subdivided into two modes as follows. Before t_0, the transformer magnetizing inductor current I_{Lm} freewheels through the secondary capacitor C_S.

Mode 1 [$t_0 \sim t_1$] : After Q is turned on at t_0, the powering path from the input to the output is formed through L_{lkg}, C_S, D_{S1}, and Q. Therefore, L_{lkg} drives the powering current and resonates with C_S. The primary current $I_{lkg}(t)$ contains this powering current and $I_{Lm}(t)$ as well. $I_{lkg}(t)$ and $I_{Lm}(t)$ are expressed as follows:

$$I_{lkg}(t) = \left(V_S + V_{Cs}(t_0) - nV_O\right)\frac{1}{Z_R}\sin\left(\omega_r(t-t_0)\right) + I_{Lm}(t-t_0)$$

$$Z_R = n_p\sqrt{\frac{L_{lkg}}{C_S}}, \quad \omega_r = \frac{n_p}{\sqrt{L_{lkg}C_S}} \tag{1}$$

$$I_{Lm}(t) = I_{Lm}(t_0)\cos\left(\omega_m(t-t_0)\right) + \left(n_pV_O - n_pV_{Cs}(t_0)\right)\frac{1}{Z_M}\sin\left(\omega_m(t-t_0)\right)$$

$$, \; Z_M = n_p\sqrt{\frac{L_M}{C_S}}, \quad \omega_m = \frac{n_p}{\sqrt{L_MC_S}} \tag{2}$$

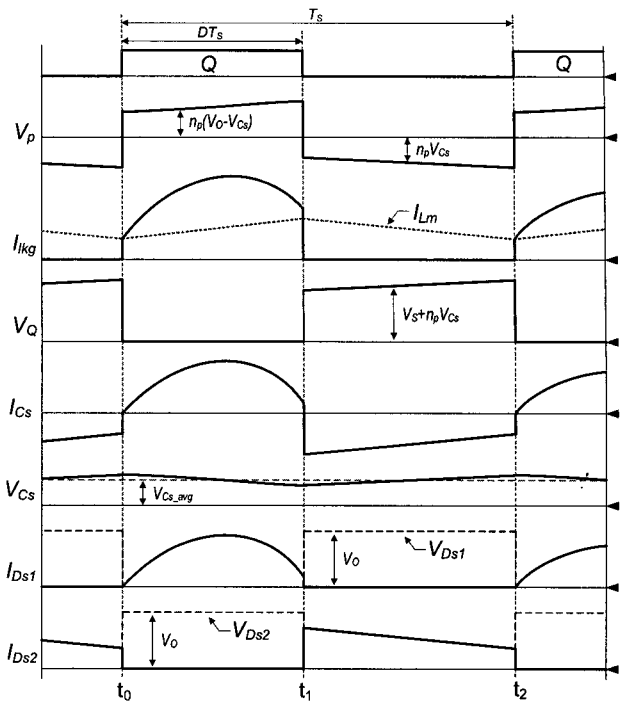

Fig. 3 Key waveforms of proposed converter

Provided that the ripple of $V_{Cs}(t)$ is small enough $I_{Lm}(t)$ can be approximated as (3), where V_{Cs_avg} means the average value of $V_{Cs}(t)$.

$$I_{Lm}(t) \approx I_{Lm}(t_0) + \frac{\left(n_pV_O - n_pV_{Cs\_avg}\right)(t-t_0)}{L_M} \tag{3}$$

The real powering current which transfers the power from the input to the output is the difference between $I_{lkg}(t)$ and $I_{Lm}(t)$. This current flows to the output through C_S and D_{S1} and is expressed as follows:

$$I_{Ds1}(t) = n_p\left(V_S + V_{Cs}(t_0) - n_pV_O\right)\frac{1}{Z_R}\sin\left(\omega_r(t-t_0)\right) \tag{4}$$

Mode 2 [$t_1 \sim t_2$] : After Q is turned off at t_1, $I_{lkg}(t)$ is rapidly decreased to zero since the primary current path is blocked. Therefore $I_{Lm}(t)$, which used to flow in the primary, now flows though C_S and D_{S2} of the secondary. Hence, $nV_{Cs}(t)$ is applied to L_m reversely and the reset of the transformer is achieved.

$I_{Lm}(t)$ is expressed as (5). Provided that the ripple of $V_{Cs}(t)$ is small enough $I_{Lm}(t)$ can be approximated as (6).

$$I_{Lm}(t) = I_{Lm}(t_1)\cos(\omega_m(t-t_1)) + \frac{n_p V_{Cs}(t_1)}{Z_M}\sin(\omega_m(t-t_1)) \quad (5)$$

$$I_{Lm}(t) \cong I_{Lm}(t_1) - \frac{n_p V_{Cs\_avg}(t-t_1)}{L_M}. \quad (6)$$

In this mode, the voltage spike of $V_Q(t)$ at the turn-off instant by L_{lkg}'s energy is not considered.

At t_2, one period is completed and the same operation is repeated.

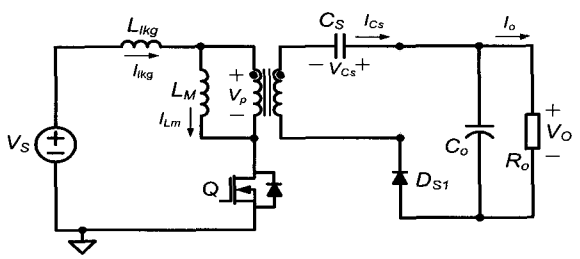

(a)

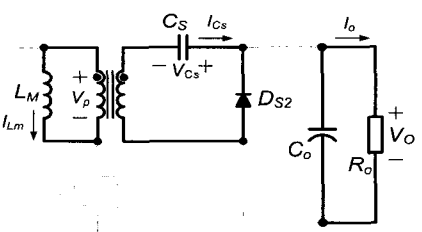

(b)

Fig. 4 Topological states of operational mode. (a) Mode 1 (t_0~t_1). (b) Mode 2 (t_1~t_2)

3. Characteristics

In this section the characteristics of the proposed converter are presented and compared with the flyback converter.

3.1 DC conversion ratio

The voltage-second balance across L_M can be expressed as (7) using V_{Cs_avg}, then the relationship between V_{Cs_avg} and V_O is expressed as (8).

$$D(n_p V_O - n_p V_{Cs\_avg}) = (1-D) n_p V_{Cs\_avg} \quad (7)$$

$$V_{Cs\_avg} = DV_O \quad (8)$$

In mode 1 the average current flows through C_S, which is the same as the load current I_O. Therefore, the voltage ripple of $V_{Cs}(t)$, ΔV_{Cs} can be expressed as (9).

$$\Delta V_{Cs} = \frac{I_O T_S}{C_S} = \frac{V_O T_S}{R_O C_S} \quad (9)$$

Since the averaging current of I_{Ds1} is equal to I_O, it can be expressed as (10). $V_{Cs}(t_0)$ is expressed as (11) from (8) and (9).

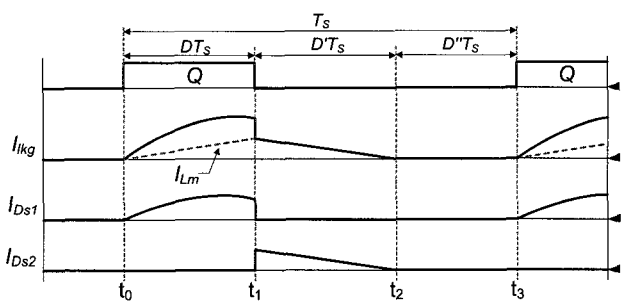

Fig. 5 DCM waveforms of proposed converter

$$I_O = \frac{V_O}{R_O} = \frac{C_S}{n_p T_S}\left(V_S + n_p V_{Cs}(t_0) - n_p V_O\right)\left(1-\cos(\omega_r DT_S)\right) \quad (10)$$

$$V_{Cs}(t_0) = V_{Cs\_avg} + \frac{\Delta V_{Cs}}{2} = DV_O + \frac{V_O T_S}{2R_O C_S} \quad (11)$$

By substituting (11) to (10), the input-output voltage conversion ratio is obtained as follows:

$$\frac{V_O}{V_S} = \frac{1}{n_p[A+1-D]} \quad (12)$$

$$A = \frac{T_S}{R_O C_S}\left(\frac{1}{2} - \frac{1}{1-\cos(\omega_r DT_S)}\right) \quad (13)$$

If the value of 'A' is small enough, (12) can be approximated as (14) like the boost conversion ratio and V_{Cs_avg} also can be approximated as (15). In other words, provided that the voltage applied to L_{lkg} is small enough to be ignored, the voltage applied to L_M would be similar to that of the flyback converter. Therefore, V_{Cs} can be expressed as (15). In a similar way, since V_S, V_{Cs}, and V_O are connected in a series when in a switch conducting state, V_O can be approximated as (14).

$$\frac{V_O}{V_S} \approx \frac{1}{n_p(1-D)} \tag{14}$$

$$V_{Cs\_avg} \approx \frac{DV_S}{n_p(1-D)} \tag{15}$$

Since the reset action of L_M is similar to the flyback converter, it also can be operated in the discontinuous conduction mode (DCM) at the light load as shown in Fig. 5, i.e., I_{Ds2} can be decreased to zero during the switch-off state. In DCM, the DC-conversion ratio of the proposed converter can be approximated as follows:

$$\frac{V_O}{V_S} \approx \frac{1+\sqrt{1+2n_p^2 D^2 T_S R_O / L_M}}{2n_p} \tag{16}$$

As presented in (14) the DC-conversion ratio of the proposed converter in continuous conduction mode (CCM) is mainly dependent on the duty, not on the load. Therefore, the duty is rarely changed under the load variation. On the other hand, as shown in (16), the DC-conversion ratio in DCM is strongly affected by the load as well. Thus, the load variation in DCM changes the operating duty as other converters.

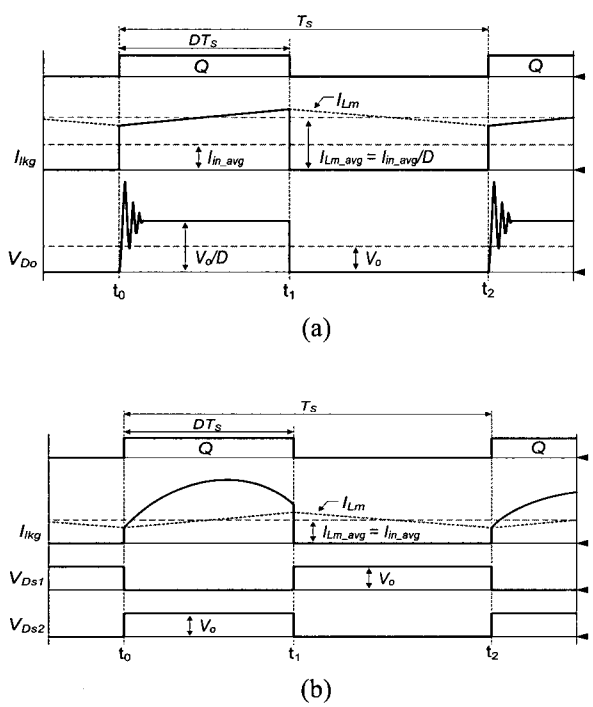

Fig. 6 Comparison between (a) flybcak converter and (b) proposed converter

3.2 Transformer

In the proposed converter, the reset of the transformer is automatically achieved by V_{Cs} without an auxiliary circuitry like the flyback converter. However, this reset operation causes additional conduction loss in the secondary since the reflected magnetizing current flows through D_{S2}.

In general, a transformer size is considerably influenced by the offset of the transformer magnetizing current. That is, a large offset current increases a transformer size [6,7].

Therefore, the transformer size of the flyback converter is inevitably large and it is one of the main drawbacks of the flyback converter that limits its rated power. Fig. 6 presents the transformer primary current I_{lkg} and magnetizing current I_{Lm} of the proposed converter and flyback converter, where I_{in_avg}, means the average of input current. In the proposed converter, the average current of magnetizing current I_{Lm_avg} is the same as I_{in_avg}. On the other hand, I_{Lm_avg} is equal to I_{in_avg}/D in the flyback converter. That is, the proposed converter has a lesser offset of the magnetizing current, which can result in a smaller transformer size. However, if both converters are designed to be operated in DCM, the transformer size would be similar.

3.3 Voltage stress of devices

Using (14) the voltage stress of the proposed converter can be approximated as $V_S/(1-D)$ and is the same as that of the flyback converter. In both converters, a RCD-snubber is required to prevent the voltage overshoot and ringing caused by L_{lkg} as can be seen in Figs. 1 and 2.

Fig. 6 shows the voltage waveform of the secondary diode. In the flyback converter, the voltage stress of the secondary diode is V_O/D and a snubber is required to damp the ringing caused by L_{lkg}. On the other hand, in the proposed converter the voltage stress of secondary diodes D_{S1} and D_{S2} are clamped to V_O since the two diodes are connected in a series across the output V_O. Therefore, it has basically less voltage stress than the flyback converter; moreover no snubber is required.

3.4 Current stress of devices

The current stresses of the proposed converter are basically higher than those of the flyback converter

Table 1 Comparison of Device Stresses between Flyback converter and Proposed converter

	Flyback converter	Proposed converter
I_{Lm_avg}	$\frac{I_{in\_avg}}{D}$	I_{in_avg}
I_{Q_peak}	$\frac{I_{in\_avg}}{D}+\frac{DV_ST_S}{2L_M}$	$\frac{1}{Z_R}\left[V_S+V_O\left(D+\frac{T_S}{2R_OC_S}-n_p\right)\right]+I_{in\_avg}$
V_Q	$\frac{V_S}{1-D}+\alpha$	$\frac{V_S}{1-D}+\alpha$
I_{D_peak}	$\frac{I_O}{1-D}+\frac{n_fDV_ST_S}{2L_M}$	D_{s1}: $\frac{n_p}{Z_R}\left[V_S+V_O\left(D+\frac{T_S}{2R_OC_S}-n_p\right)\right]$ D_{s2}: $\frac{I_O}{1-D}+\frac{n_pDV_ST_S}{2L_M}$
V_D	$\frac{V_O}{D}+\alpha$	V_O

because of the resonance between L_{lkg} and C_S. From (4) and (11) the peak current of I_{Ds1} is obtained as follow.

$$I_{Ds1\_peak}=\frac{n_p}{Z_R}\left[V_S+V_O\left(D+\frac{T_S}{2R_OC_S}-n_p\right)\right] \tag{17}$$

By the current-second balance of C_S, the average of I_{Ds2} is equal to the average of I_{Ds1}. I_{Ds2} is the reflected magnetizing current, thus its peak current is dependent on the magnetizing inductance. The peak current of I_{Ds2} can be approximated as (18) and is similar to that of the flyback converter.

$$I_{Ds2\_peak}=\frac{I_O}{1-D}+\frac{n_pDV_ST_S}{2L_M} \tag{18}$$

Provided that the ripple current of I_{Lm} is small, the peak switch current I_{Q_peak} can be approximated as (19) using (1).

$$I_{Q\_peak}=\frac{1}{Z_R}\left[V_S+V_O\left(D+\frac{T_S}{2R_OC_S}-n_p\right)\right]+I_{in\_avg} \tag{19}$$

3.5 Switch turn-off loss and snubber loss

The switch turn-off loss is mainly determined by the switch current at the instant of turn-off. As can be seen in Fig. 6, the switch current of the proposed converter at the instant of turn-off is less than that of the flyback converter by the help of resonance between L_{lkg} and C_S. Therefore, the proposed converter has less turn-off loss.

In the case of using a RCD-snubber in the primary as shown in Figs. 1 and 2, the loss dissipated by the snubber is dependent on the energy stored in L_{lkg} [8]. That is, I_{lkg} at the instant of turn-off mainly determines the loss. Therefore, the proposed converter has also less dissipation by the snubber compared with the flyback converter.

Table 1 shows the comparison of device stress between the flyback converter and proposed converter, where I_{D_peak} and V_D mean the peak current and voltage stress of secondary diode, respectively, and ' α ' means the additional voltage stress caused by the voltage spike and ringing. Provided that the flyback converter and proposed converter are operated in same duty, the relationship of turn ratio is expressed as follows:

$$Dn_p=n_f \tag{20}$$

To be brief, although the proposed converter has more components and additional conduction loss of the secondary, its transformer size, switch turn-off loss, and voltage stress of diodes are significantly reduced compared with the conventional flyback converter. Moreover, no additional snubber across the secondary diodes is required.

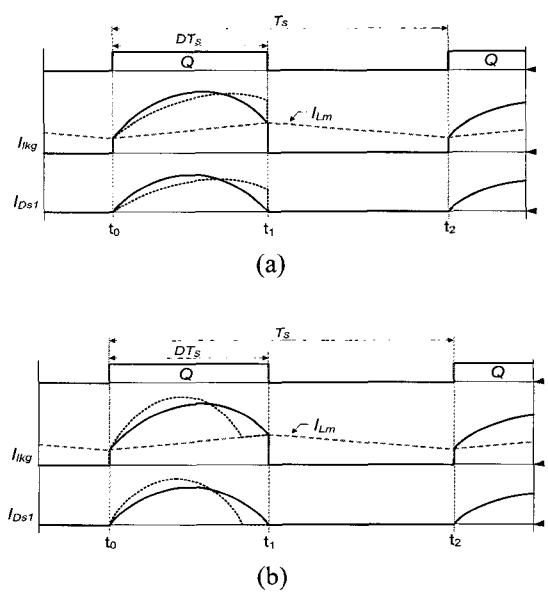

Fig. 7 Comparison of current waveform. (a) $T_R/2 > DT_S$. (b) $T_R/2 < DT_S$

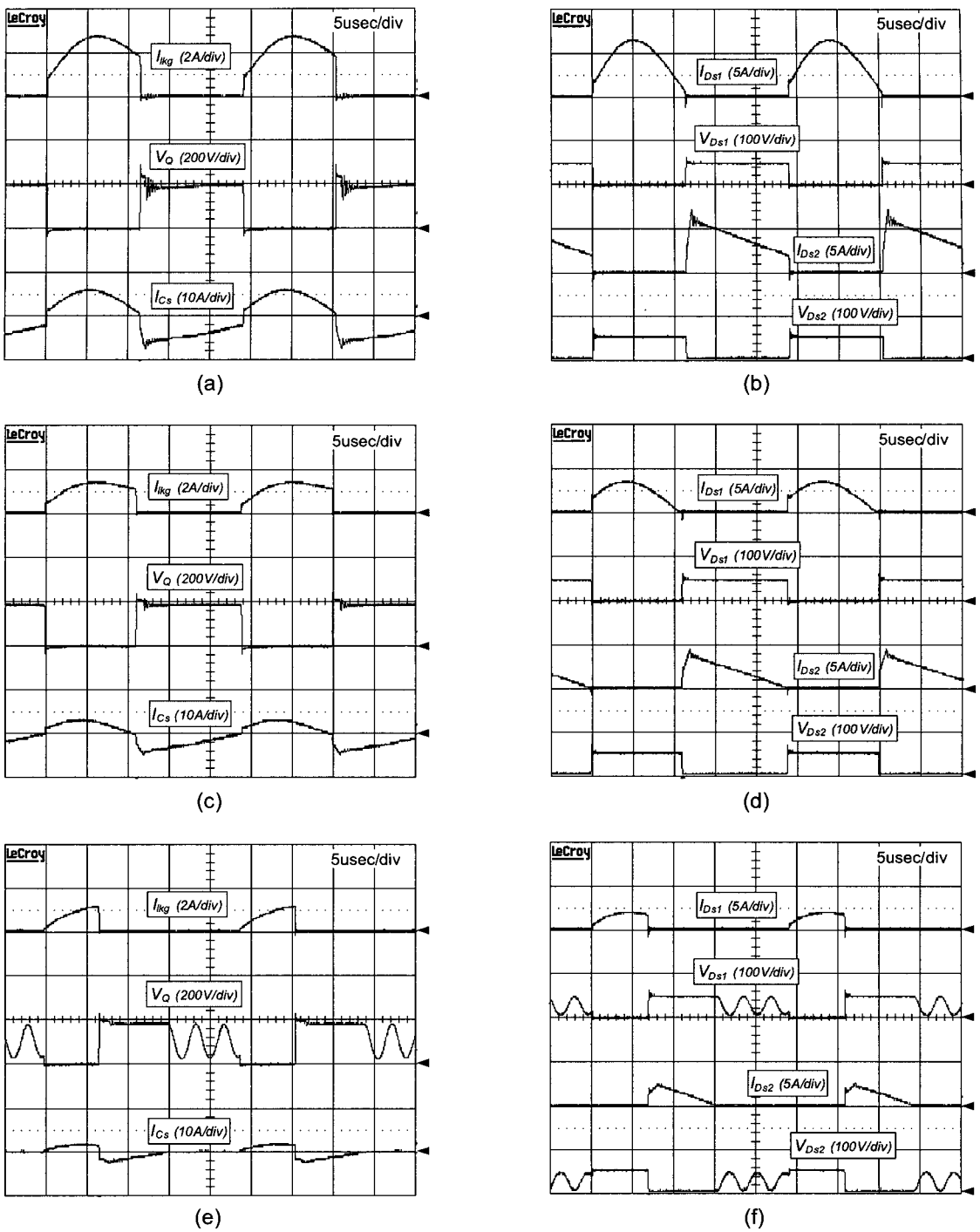

Fig. 8 Experimental waveforms. (a) I_{lkg}, V_Q, and I_{Cs} at full load. (b) I_{Ds1}, V_{Ds1}, I_{Ds2}, and V_{Ds2} at full load. (c) I_{lkg}, V_Q, and I_{Cs} at 50% load. (d) I_{Ds1}, V_{Ds1}, I_{Ds2}, and V_{Ds2} at 50% load. (e) I_{lkg}, V_Q, and I_{Cs} at 20% load. (f) I_{Ds1}, V_{Ds1}, I_{Ds2}, and V_{Ds2} at 20% load.

4. Design Consideration

4.1 Selecting duty and turn ratio

The primary device stress of the proposed converter is similar to that of the flyback converter as shown in Table 1 since it also utilizes only one switch. Generally,

single-switch type converters such as the flyback or forward converters suffer from high voltage stress to reset the transformer as its duty increases. On the other hands, a smaller duty increases the current stress of the switch. Therefore, the duty and transformer turn ratio of the proposed converter are chosen to accommodate as low a voltage rating for the switch as possible while having a reasonable current stress of the switch using an adequate trade-off.

4.2 Selecting resonant capacitor C_S

Fig. 7 shows the current waveform of the proposed converter, where T_R is the resonant period between L_{lkg} and C_S, i.e., $T_R = 1/2\pi\omega_r$. The proper selection of T_R can improve the converter performance. In the case of $T_R/2>DT_S$, the current stress of device can be reduced; however, the switch turn-off loss is increased. On the other hands, in the case of $T_R/2<DT_S$ the switch turn-off loss is reduced and D_{S1} achieves zero-current-switching (ZCS) turn-off which minimize the reverse recovery of the diode. However, the current stress and conduction loss of the devices are rather increased. Therefore, T_R is selected in the midpoint as (21) to achieve ZCS of the diode while minimizing the switch turn-off loss as presented in the solid line of Fig. 7.

$$\frac{T_R}{2} = DT_S \tag{21}$$

To minimize the switch turn-off snubber loss, the smaller L_{lkg} is desirable. Thus, once L_{lkg} is determined from the fabricated transformer, L_{lkg} is set as it is and C_S can be selected as follows:

$$C_S = \frac{4\left(\pi n_p DT_S\right)^2}{L_{lkg}} \tag{22}$$

The condition (21) can be maintained as long as the converter is operated in CCM. However, at a light load where the converter is operated in DCM, the duty is decreased and the condition (21) cannot be guaranteed any more.

4.3 Selecting transformer magnetizing inductor L_M

In the proposed converter, the effect of L_M is similar to that of the flyback converter. The large inductance of L_M resulting in a small current ripple of I_{Lm} can reduce the switch turn-off loss and the current stress of D_{S2}. Moreover, the large inductance enlarges a CCM range which guarantees the condition (21). However it increases the transformer size. Therefore, a reasonable trade-off between these factors is required.

5. Experimental Results

The prototype of the proposed converter has been built with the following specifications: input voltage V_S = 100V, output voltage V_O = 48V, output power P_O = 100W, switching frequency f_S = 42kHz, switch Q: FQP17N40, secondary diodes D_{S1} and D_{S2}: 30CTQ060, transformer T: EER3435, turn ratio n_p=56/15, transformer leakage inductance L_{lkg}: 20uH, transformer magnetizing inductance L_m:950uH, and resonant capacitor C_S: 11uF, where a RCD-snubber (R_C=10kΩ) is employed across Q.

Figs. 8 (a) and (b) show the key experimental waveforms of the proposed converter at full load condition. It can be seen that I_{lkg} drives the powering current with the resonance between L_{lkg} and C_S, and it decreases I_{lkg} at the instant of switch turn-off. Moreover, it turns-off the secondary diode D_{S1} smoothly, which minimize the reverse recovery. The voltage stresses of D_{S1} and D_{S2} are effectively limited by V_O without additional RC-snubbers.

Figs. 8(c) and (d) show the experimental waveforms at the 50% load condition, and Figs. 8(e) and (f) do at the 20% load condition. In the 50% load condition, it is still operated in the CCM, therefore the duty is rarely changed and ZCS turn-off of D_{S1} is still achieved. On the other hands, in the 20% load condition, it is operated under the DCM. Thus, the duty is considerably reduced, which increases I_{lkg} at the turn-off instant and loses ZCS turn-off condition of D_{S1}. Instead, D_{S2} is turned off smoothly.

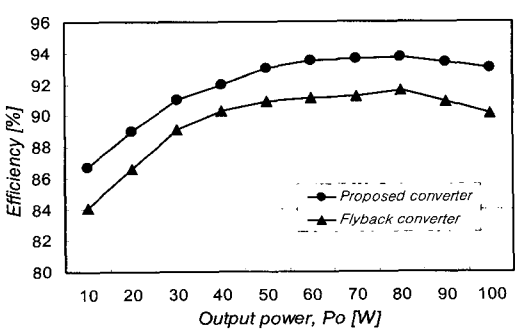

Fig. 9 Measured efficiency

Fig. 9 shows the measured efficiency of the proposed converter and flyback converter. Since the proposed converter has the reduced turn-off loss, the reduced RCD-snubber loss and no dissipative snubber in the secondary, it can achieve a higher efficiency than the flyback converter along a wide load range.

6. Conclusion

A new single switch isolated converter is proposed, which utilizes the transformer leakage inductor to drive the powering current instead of a large inductor. The proposed converter has a reduced transformer size, reduced switch turn-off loss, and reduced voltage stress on the secondary diodes compared with the flyback converter. Moreover, no dissipative snubber across the secondary diodes and no additional transformer reset circuit are required. Therefore, it features a simple structure, low cost, and high efficiency promise for small power applications.

References

[1] J. A. Sabate, V. Vlatkovic, R. B. Ridley, F. C. Lee, and B. H. Cho, "Design consideration for high-voltage high-power full-bridge zero-voltage-switched PWM converter," in Proc. IEEE APEC, 1990, pp. 275-284.

[2] Paul Imbertson and Ned Mohan, "Asymmetrical duty cycle permits zero switching loss in PWM circuits with no conduction loss penalty," IEEE Trans. Industry Application, Vol. 29, No. 1, 1993, pp. 121-125.

[3] A. Acik and I. Cadirci, "Active clamped ZVS forward converter with soft-switched synchronous rectifier for high efficiency, low output voltage applications," IEE Proc. Electric Power Application, Vol. 150, No. 2, 2003, pp. 165-174.

[4] M. T. Zhang, M. M. Javanovic, and F. C. Lee, "Design considerations and performance evaluations of synchronous rectification in flyback converters," IEEE Trans. Power Electronics, Vol. 13, No. 3, 1998, pp. 538-546.

[5] T. H. Chen, W. L. Lin, and C. M. Liaw, "Dynamic modeling and controller design of flyback converter," IEEE trans. Aerospace and Electronic System, Vol. 35, No. 4, 1999, pp. 1230-1239.

[6] A. I. Pressman, Switching Power Supply Design. New York: McGraw-Hill, 1991.

[7] Xiangiun Zhang, Hankui Liu, and Dianguo Xu, " Analysis and design of the flyback transformer," in Proc. IEEE IECON, 2003, pp. 715-719.

[8] Hang-Seok Choi, "Application note AN4137 – Design guide lines for off-line flyback converters using fairchild power switch (FPS)," Fairchild Semiconductor Corporation, 2003.

Ki-Bum Park was born in Korea in 1981. He received his B.S. and M.S. degrees in Electrical Engineering from the Korea Advanced Institute of Science and Technology (KAIST), Daejeon, Korea, in 2003 and 2005, respectively, where he is currently working toward his Ph.D. degree. His main research interests are DC/DC converter, power-factor-correction (PFC) AC/DC converters, driver circuits of plasma display panel (PDP), backlight inverters of LCD TV and battery equalizer.

Chong-Eun Kim received his B.S. degree in Electrical Engineering from Kyungpook National University, Daegu, Korea, in 2001. In 2003, he received his M.S. degree in Electrical Engineering from Korea Advanced Institute of Science and Technology (KAIST), Daejeon, Korea, where he is currently working toward his Ph.D. degree. His main research interests are DC/DC converters, power-factor-correction (PFC) AC/DC converters, soft switching technique, plasma display panel (PDP), and digital audio amplifiers.

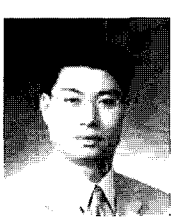

Gun-Woo Moon received his M.S. and Ph.D. degrees in Electrical Engineering from the Korea Advanced Institute of Science and Technology (KAIST), Daejeon, in 1992 and 1996, respectively. He is currently an Associate Professor in the department of Electrical Engineering, KAIST. His research interests include modeling, design and control of power converters, soft-switching power converters, resonant inverters, distributed power systems, power-factor correction, electric drive systems, driver circuits of plasma display panels, and flexible ac transmission systems. Dr. Moon is a member of the Korean Institute of Power Electronics (KIPE), Korean Institute of Electrical Engineers (KIEE), Korea Institute of Telematics and Electronics (KITE), Korea Institute of Illumination Electronics and Industrial Equipment (KIIEIE), and Society for Information Display (SID).

Myung-Joong Youn was born in Seoul, Korea in 1946. He received his B.S. degree from Seoul National University, Seoul, in 1970 and his M.S. and Ph.D. degrees in electrical engineering from the University of Missouri, Columbia, in 1974 and 1978, respectively. In 1978, he joined the Air-Craft Equipment Division, General Electric Company in Erie, PA, where he was an Individual Contributor on Aerospace Electrical System Engineering. Since 1983, he has been a professor at the Korea Advanced Institute of Science and Technology (KAIST), Daejeon. His research activities are in the areas of power electronics and control, which include the drive systems, rotating electrical machine design, and high-performance switching regulators. Dr. Youn is a member of the Institution of Electrical Engineers, U.K., the Korean Institute of Power Electronics (KIPE), the Korean Institute of Electrical Engineers (KIEE), and the Korea Institute of Telematics and Electronics (KITE).